Common Anesthetic-binding Site for Inhibition of Pentameric Ligand-gated Ion Channels

Monica N. Kinde, Ph.D., Weiming Bu, Ph.D., Qiang Chen, Ph.D., Yan Xu, Ph.D., Roderic G. Eckenhoff, M.D., Pei Tang, Ph.D.

ABSTRACT

Background: Identifying functionally relevant anesthetic-binding sites in pentameric ligand-gated ion channels (pLGICs) is an important step toward understanding the molecular mechanisms underlying anesthetic action. The anesthetic propofol is known to inhibit cation-conducting pLGICs, including a prokaryotic pLGIC from *Erwinia chrysanthemi* (ELIC), but the sites responsible for functional inhibition remain undetermined.

Methods: We photolabeled ELIC with a light-activated derivative of propofol (AziP*m*) and performed fluorine-19 nuclear magnetic resonance experiments to support propofol binding to a transmembrane domain (TMD) intrasubunit pocket. To differentiate sites responsible for propofol inhibition from those that are functionally irrelevant, we made an ELIC-γ-aminobutyric acid receptor ($GABA_AR$) chimera that replaced the ELIC-TMD with the α1β3$GABA_AR$-TMD and compared functional responses of ELIC-$GABA_AR$ and ELIC with propofol modulations.

Results: Photolabeling showed multiple AziP*m*-binding sites in the extracellular domain (ECD) but only one site in the TMD with labeled residues M265 and F308 in the resting state of ELIC. Notably, this TMD site is an intrasubunit pocket that overlaps with binding sites for anesthetics, including propofol, found previously in other pLGICs. Fluorine-19 nuclear magnetic resonance experiments supported propofol binding to this TMD intrasubunit pocket only in the absence of agonist. Functional measurements of ELIC-$GABA_AR$ showed propofol potentiation of the agonist-elicited current instead of inhibition observed on ELIC.

Conclusions: The distinctly different responses of ELIC and ELIC-$GABA_AR$ to propofol support the functional relevance of propofol binding to the TMD. Combining the newly identified TMD intrasubunit pocket in ELIC with equivalent TMD anesthetic sites found previously in other cationic pLGICs, we propose this TMD pocket as a common site for anesthetic inhibition of pLGICs. **(Anesthesiology 2016; 124:664-73)**

PENTAMERIC ligand-gated ion channels (pLGICs) are molecular targets of general anesthetics.[1,2] Anesthetic binding often inhibits agonist-elicited currents of cation-conducting pLGICs, such as excitatory nicotinic acetylcholine receptors (nAChRs), but potentiates functions of anion-conducting pLGICs, such as inhibitory γ-aminobutyric acid receptors ($GABA_ARs$).[1,2] To understand how general anesthetics modulate functions of pLGICs requires the knowledge of anesthetic-binding sites in these channels, especially those binding sites that render functional changes in pLGICs. A clear map for functionally relevant anesthetic sites in pLGICs will also benefit rational design of new generation anesthetics that have better specificity and fewer unwanted side effects.[3,4]

Both experimental and computational approaches have been used in the past for identifying anesthetic-binding sites.[5–19] Anesthetics have been found to bind to both the extracellular domain (ECD)[15] and the transmembrane domain (TMD)[13,14,16] in crystal structures of pLGICs. Anesthetic-binding sites in the pore and the intracellular region have also been suggested by site-directed mutagenesis,

What We Already Know about This Topic

- Pentameric ligand-gated ion channels (pLGICs) are important targets for most general anesthetics, including propofol
- Anesthetics generally inhibit cation-conducting pLGICs and potentiate anion-conducting pLGICs

What This Article Tells Us That Is New

- Using ELIC, a prokaryotic pLGIC from *Erwinia chrysanthemi*, as a model, propofol is shown to bind in a transmembrane intrasubunit pocket that overlaps anesthetic-binding sites previously identified in other pLGICs
- The functional relevance of this binding site is demonstrated by analysis of chimeric receptors, which suggests that the transmembrane intrasubunit site is a common binding site for anesthetic inhibition of cationic pLGICs

Supplemental Digital Content is available for this article. Direct URL citations appear in the printed text and are available in both the HTML and PDF versions of this article. Links to the digital files are provided in the HTML text of this article on the Journal's Web site (www.anesthesiology.org).

Submitted July 9, 2015. Accepted for publication November 30, 2015. From the Departments of Anesthesiology (M.N.K., Q.C., Y.X., P.T.), Pharmacology and Chemical Biology (Y.X., P.T.), Structural Biology (Y.X.), and Computational and Systems Biology (P.T.), University of Pittsburgh School of Medicine, Pittsburgh, Pennsylvania; and Department of Anesthesiology and Critical Care, Perelman School of Medicine, University of Pennsylvania, Philadelphia, Pennsylvania (W.B., R.G.E.).

 Anesthesiology 2016; 124:664-73

<zdoi;10.1097/ALN.0000000000001005>

electrophysiology measurements, and photoaffinity labeling.[20–24] For a given anesthetic in a particular protein, one often observes multiple anesthetic-binding sites.[5,6,9,12,25] Thus, the success of finding multiple anesthetic-binding sites has introduced a more challenging question: which specific site or sites among all those identified is responsible for functional modulation?

With the accumulation of information regarding anesthetic-binding sites in pLGICs, it becomes notable that anesthetics frequently bind to the same region of different pLGICs. For example, propofol and desflurane bound to an intrasubunit pocket in the TMD of GLIC,[10,14] a prokaryotic pLGIC from *Gloeobacter violaceus*. An intrasubunit site within the δ-subunit helix bundle of nAChRs was also found for binding propofol,[11] etomidate,[24,25] and halothane.[26] The frequent occurrence of anesthetic binding to this region raises the question as to whether a common anesthetic site exists for inhibitory modulations in cation-conducting pLGICs.

In this study, we determined a functionally relevant propofol-binding site in ELIC, a cation-conducting pLGIC from *Erwinia chrysanthemi*, that is structurally homologous to mammalian pLGICs, such as nAChRs.[27–29] Photolabeling ELIC with the light-activated derivative of propofol (AziP*m*)[30] showed multiple AziP*m*-binding sites in the ECD and an intrasubunit pocket in the TMD that overlapped with the TMD intrasubunit anesthetic site in GLIC[10,14] and nAChRs.[11,24–26] Fluorine-19 nuclear magnetic resonance (^{19}F NMR) experiments further supported propofol binding to this TMD intrasubunit pocket of ELIC in the absence, but not in the presence, of agonist. To evaluate the relevance of propofol-binding sites in the ECD and TMD to functional inhibition of ELIC, we used an ELIC-$GABA_AR$ chimera that replaced the ELIC-TMD with the α1β3$GABA_AR$-TMD. The chimera shows functional and pharmacological characteristics of α1β3$GABA_AR$, including the functional potentiation by propofol. Distinctly different responses of ELIC and ELIC-$GABA_AR$ to propofol provide supportive evidence for the functional relevance of propofol binding to the TMD. The finding of this newly identified TMD intrasubunit pocket in ELIC along with previously identified equivalent anesthetic sites in other pLGICs suggests that this TMD intrasubunit pocket is a common site for anesthetic inhibition of cationic pLGICs.

Materials and Methods

ELIC Photolabeling with AziPm and Adduct Identification

A pentameric ligand-gated ion channel from *Erwinia chrysanthemi* was expressed and purified as reported previously.[27,28,31] For photolabeling, a mixture of ELIC (1 mg/ml) and AziP*m* (50 μM) was placed in a quartz cuvette (1 mm path length) and exposed to an ultraviolet light (350 nm) for 20 min. To determine whether propofol inhibits AziP*m* binding, the same labeling procedure was also performed for ELIC photolabeling with [^{3}H]AziP*m* (50 μM) in the absence and presence of propofol (approximately 400 μM, the maximum soluble concentration). For all sample conditions, ELIC was resolved in triplicate by sodium dodecyl sulfate–polyacrylamide gel electrophoresis with Coomassie G-250 staining. Each stained band of ELIC at approximately 37 kDa was excised for adduct identification using liquid chromatography-tandem mass spectrometry (MS/MS) or for scintillation counting in the case of ELIC photolabeling with [^{3}H]AziP*m*.

For adduct identification, samples were separated using a C18 nanoLC column with a flow rate of 200 nl/min after trypsin digestion. A 60-min water–acetonitrile gradient was used in combination with the online electrospray into a Thermo LTQ linear ion trap (Thermo Scientific, USA). Raw data were acquired using XCalibur (Thermo Scientific, USA). The mass spectra were searched against the known ELIC sequence for tryptic peptide identification. Search parameters included 1 amu for parent and fragment ion tolerance, 0 to 1 missed cleavage, methionine oxidation (+15.99491) as a variable modification, and cysteine alkylation (+57.02146) as a fixed modification. Filter parameters include *Xcorr* scores of (+1 ion) 1.5, (+2 ion) 2.0, (+3 ion) 2.5, ΔCn 0.08, and peptide probability greater than 0.05. A mass modification corresponding to AziP*m* (216.076 Da) on any amino acid of every tryptic-digested peptide was then identified. The spectra of the AziP*m*-modified peptides were manually inspected for verification. On identification of modified peptides, MS/MS was used for further fragmentation and *Sequest* was used for searching b (charge retained on the *N*-terminal fragment) and y (charge retained on the *C*-terminal fragment) ions to localize the modified amino acid.

For scintillation counting, the gel bands were dissolved overnight at 60°C in sealed scintillation vials containing 350 μl of 30% hydrogen peroxide. After cooling, scintillation fluid was added to each vial for counting. Data analysis was performed using the Prism 5.0 (GraphPad, USA).

^{19}F NMR

Single-cysteine mutations were introduced to either M265 or F308 of ELIC after mutating native C300 and C313 to alanine and serine, respectively, using the QuikChange Lightening Mutagenesis Kit (Agilent Technologies, USA). Expression and purification of the ELIC constructs were conducted after the same protocols as those used for ELIC reported previously.[27,28,31] 2,2,2-Trifluoroethanethiol (TET), a widely used probe for ^{19}F NMR,[31,32] was covalently labeled to M265C or F308C as described previously.[32,33] Briefly, we added approximately 70-fold excess of TET to the purified ELIC, shook the mixture at room temperature for 4 h, and then shook it continually at 4°C overnight to complete the reaction. Residual-free TET was removed by dialysis and subsequent size exclusion chromatography (Superdex 200 10/300GL column; GE Healthcare, USA). The fraction corresponding to the pentameric ELIC was collected and concentrated for nuclear magnetic resonance (NMR) measurements. Each NMR sample typically contained 50 to 100 μM ELIC, 1 mM lipids (asolectin; Sigma, USA),

approximately 8 mM (approximately 0.4%) *n*-undecyl-β-D-maltoside (Anatrace, USA), 75 mM NaCl, 25 mM sodium phosphate at pH 7, and 10% D_2O for the lock of deuterium signals in NMR experiments. Spectra for desensitized ELIC were collected in the presence of the agonist propylamine with a concentration of 18 mM. Spectra for the determination of propofol-binding effects were collected after adding 120 μM propofol to the ELIC samples.

^{19}F NMR spectra were recorded on a Bruker-BioSpin Avance 600 spectrometer (Bruker Corporation, USA) (^{19}F frequency 564.6 MHz at 14 T). The chemical shifts were externally referenced to trichlorofluoromethane at 0.0 ppm. The data collection parameters included a 1-s recycle delay, a 30-ppm spectral window with 8,192 complex points, and approximately 50,000 scans. The data were processed with an exponential function of 50 Hz line broadening and zero-filled to 32,768 points before Fourier transformation.[31] Line shape analysis was performed using MestReNova v8.0.1-10878 software (Mestrelab Research S.L., Spain). ^{19}F NMR spectra for both residue sites were collected at 283, 293, and 303 K. Spectrometer temperatures were calibrated using a methanol standard.

Functional Measurements

Functional measurements were performed on *Xenopus laevis* oocytes expressing ELIC, its mutants, and the ELIC-$GABA_A$R chimera. The procedures involving *X. laevis* oocytes were approved by the University of Pittsburgh Institutional Animal Care and Use Committee, Protocol 14114745. The vector pCMV-mGFP Cterm S11 Neo Kan (Theranostech, USA) was used for the insertion of DNA-encoding ELIC downstream of a T7 promoter. Single-cysteine mutations were done using the same method as that used for the NMR samples and confirmed by DNA sequencing. The ELIC-$GABA_A$R chimeras were constructed using overlapping polymerase chain reaction by fusing the ECD of ELIC ending at R199 with the TMD and intracellular loop of the α1$GABA_A$R starting at K222 or the β3$GABA_A$R starting at N217. The resulting constructs were subcloned downstream of a T7 promoter in the vector pCMV-mGFP Cterm S11 Neo Kan (Theranostech) and confirmed by DNA sequencing. RNA preparation, channel expression in *X. laevis* oocytes, and electrophysiology measurements were performed as previously reported.[8,15,28,29] To ensure ELIC's functionality after TET labeling, the purified TET-labeled ELIC was reconstituted into lipid vesicles[6] and injected into oocytes (50 nl; 2 mg/ml protein) for functional measurements. A holding potential of −60 mV was applied to clamp oocytes. The recording solution was prepared at pH 7.0, containing 130 mM NaCl, 10 mM HEPES, 0.1 mM Ca^{2+}, and the desired concentrations of ligands (agonist, propofol, or AziP*m*). For each construct, the data were collected from n ≥ 5 oocytes and fit to the Hill equation for EC_{50} or half maximal inhibitory concentration (IC_{50}) values. Error bars in the dose–response curves represent SEM. We used Clampex 10 (Molecular Devices, USA) for data collection and processing and Prism 5.0 (GraphPad) for nonlinear regressions.

Molecular Dynamic Simulations

Propofol docking to ELIC was done with the AUTODOCK 4.2.6 program.[34] Docking grids were generated that encompassed the residues identified by the photolabeling experiment. Two hundred fifty docking structures were generated. Propofol molecules with representative orientations at individual sites were chosen for molecular dynamic (MD) simulations. NAMD2.9[35] and the CHARMM36 force field[36] were used for MD simulations of three systems: apo, propofol bound to the sites in the ECD, and propofol bound to the sites in the TMD. Each system was prepared with a crystal structure of ELIC (pdb: 3RQU),[28] which was embedded in a fully hydrated and pre-equilibrated 1-palmitoyl-2-oleoyl-sn-glycero-3-phosphocholine lipid bilayer. After energy minimization and equilibration using the protocol reported previously,[17,28] each system was simulated at a constant pressure (1 atm) and temperature (310 K). Other simulation parameters include 2 fs per time step, particle mesh Ewald[37] long-range electrostatic interactions, 12 Å cutoff for nonbonded interactions, calculating bonded and nonbonded interactions every time step, electrostatic interactions every two time steps, and hexagonal periodic boundary conditions with the dimensions 108 Å × 108 Å × 126 Å. Two parallel simulations were conducted for each system, and each simulation lasted for at least 100 ns.

Statistical Analysis

For statistical analysis, the data from the photolabeling and functional measurements were collected in triplicate and n ≥ 5 oocytes, respectively. The statistical analysis was performed using Prism 5.0 (GraphPad, USA). Two-tailed *t* test analysis was used to determine the statistical significance with a *P* value less than 0.05. Channel current responses to agonist or anesthetics were plotted against respective concentrations. The dose–response data were fit to the Hill equation using nonlinear regression to obtain either EC_{50} or IC_{50} values and the Hill slopes (n_H). These values are presented as mean ± SEM.

Results

Functional State–dependent Photolabeling of a Propofol Analog to ELIC

To identify propofol-binding sites in ELIC, we labeled ELIC with AziP*m*,[30] a photoactivatable analog of propofol. AziP*m* is known to retain propofol's *in vivo* activity and modulation of $GABA_A$ receptors.[30] It also retains propofol's inhibitory effect on GLIC and labels residues in crystallographically revealed propofol-binding sites in GLIC[10] and apoferritin.[30] For ELIC, we found that propofol and AziP*m* similarly inhibit the current elicited by the agonist propylamine (fig. 1A). The results assure the suitability of AziP*m* for the determination of propofol-binding sites in ELIC.

Photolabeling of AziP*m* to ELIC was performed in the absence and presence of the agonist, which correspond to the closed and desensitized states of ELIC, respectively. Liquid

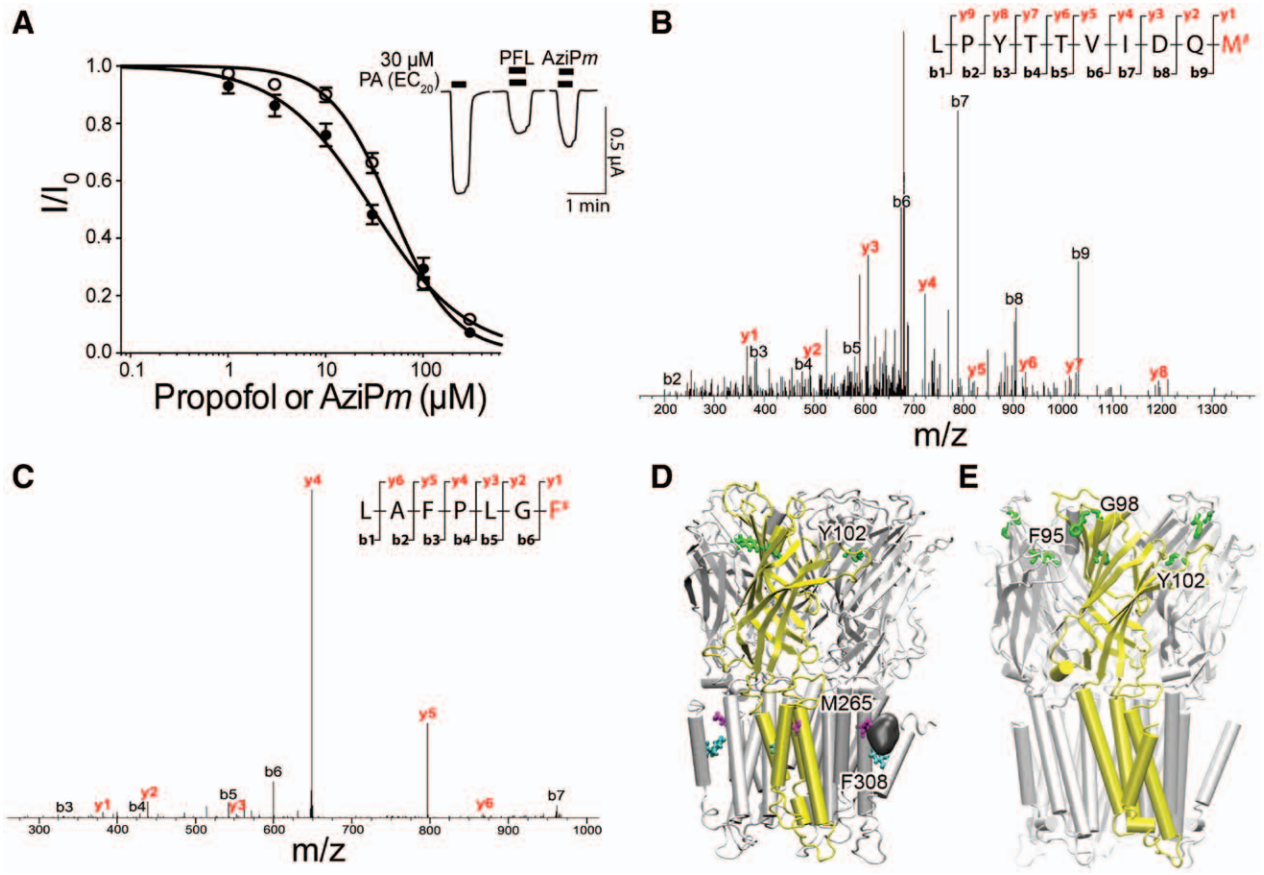

Fig. 1. The light-activated derivative of propofol (AziP*m*)-binding sites in different functional states of ligand-gated ion channel *Erwinia chrysanthemi* (ELIC). (*A*) Dose–response inhibition curves of ELIC with propofol (●) or AziP*m* (○). IC_{50} values for propofol and AziP*m* are 30.2 ± 1.1 μM and 47.1 ± 1.1 μM (n ≥ 5 oocytes), respectively. The data were fit to the Hill equation and error bars represent SEM. The *inset* shows representative traces of ELIC currents elicited by propylamine and inhibited by propofol and AziP*m*. Representative tandem mass spectra spectra showing the peptides containing the AziP*m*-adducted residues (*B*) M265 and (*C*) F308. Note that the b ion or y ion is classed if the charge is retained on the *N*-terminal or the *C*-terminal peptide fragment, respectively. A subscript indicates the number of residues in the peptide fragment. AziP*m*-bound peptide fragments are shown as *insets* with adduct sites denoted in *red*. (*D*) The ELIC structure showing AziP*m*-labeled residues in the resting state: Y102 (*green*) in the extracellular domain (ECD), M265 (*magenta*), and F308 (*cyan*) in the transmembrane domain (TMD). The TMD intrasubunit binding pocket lined by M265 and F308 is highlighted in *gray*. (*E*) In the presence of agonist (a desensitized state), AziP*m* labeled only the ECD residues: F95, G98, and Y102 (*green*). PA = propylamine; PFL = propofol.

chromatography/MS analysis and MS/MS spectra of the trypsin-digested samples showed peptides with a 94% coverage of ELIC amino acids in both resting and desensitized states (fig. S1, Supplemental Digital Content 1, http://links.lww.com/ALN/B239). Residues photolabeled by AziP*m* were identified by searching ELIC peptides for a modification of 216.076 Da, the photoactivated mass of AziP*m*. Figure 1, B and C shows representative MS/MS spectra for the identified peptides containing AziP*m*-labeled M265 and F308, respectively. Supplemental Digital Content 1 (tables S1A and S1B), http://links.lww.com/ALN/B239, shows a detailed analysis for the detected b and y ions reported in figure 1, B and C. MS/MS spectra of other AziP*m*-labeled ELIC peptides are provided in figure S2 (Supplemental Digital Content 1, http://links.lww.com/ALN/B239). Because 94% of the ELIC sequence was recovered in the mass analysis, it is possible but unlikely that there exist AziP*m*-labeled sites other than those reported here. Photolabeling performed under the resting-state condition revealed AziP*m* binding to two residues in the TMD, M265 in TM3 and F308 in TM4, and also the residue Y102 in the ECD (fig. 1D). In contrast, for photolabeling performed in the presence of agonist, a presumed desensitized condition, AziP*m* labeled residues F95, G98, and Y102 in the ECD but no residue in the TMD (fig. 1E). The data suggest that AziP*m* binding to the TMD favors the resting state of ELIC. Moreover, the two photolabeled residues in the TMD (M265 and F308) line an intrasubunit pocket (fig. 1D) that is homologous to the previously reported anesthetic-binding pocket (fig. S3, Supplemental Digital Content 1, http://links.lww.com/ALN/B239) in GLIC[10,14] and in nAChRs.[5,7,11,24–26] The frequent observation of anesthetic binding to this site

suggests that it may be a common site for anesthetic binding and inhibition of cationic pLGICs.

We also labeled ELIC with [^{3}H]AziP*m* in the absence and presence of propofol. The results (fig. S4, Supplemental Digital Content 1, http://links.lww.com/ALN/B239) show that the [^{3}H]AziP*m* photolabeling was significantly inhibited by the presence of propofol (P = 0.0053) and suggest that AziP*m* and propofol share the same binding site.

Propofol Binding to the TMD Intrasubunit Pocket in ELIC

Our photolabeling results indicate propofol binding to the TMD intrasubunit pocket in the resting state of ELIC. Although AziP*m* has a similar inhibitory effect as propofol on ELIC, they are nevertheless not identical. Therefore, we further performed ^{19}F NMR to determine whether propofol binds to the same site as AziP*m* in the TMD as identified by photolabeling. ^{19}F NMR is a sensitive method that has been widely used to determine changes in protein structures and dynamics induced by ligand binding.[31,32,38]

For ^{19}F signal detection, we made single-cysteine constructs (M265C and F308C) for covalently tagging ELIC with TET, a commonly used probe for ^{19}F NMR.[31,32] The functions of the single-cysteine constructs and the TET-labeled ELIC were ensured by two-electrode voltage clamp measurements on *X. laevis* oocytes expressing the single-cysteine ELIC (fig. S5A, Supplemental Digital Content 1, http://links.lww.com/ALN/B239) and the TET-labeled ELIC that was reconstituted into lipid vesicles and directly injected into oocytes (fig. S5B, Supplemental Digital Content 1, http://links.lww.com/ALN/B239).

^{19}F NMR spectra (fig. 2) were collected for each construct in the absence and presence of propofol in the presumed resting (without agonist) and desensitized (with agonist) states. In the resting state, a single ^{19}F NMR peak with a narrow linewidth was observed for both residues (fig. 2, A and B, blue). Residues readily accessible to solvent tend to have a single narrow peak, and the ^{19}F NMR peak linewidth reflects the side-chain mobility.[31] A decrease in the side-chain movement would cause an increase in the ^{19}F NMR peak linewidth. This increase in linewidth was observed after we added the agonist propylamine to ELIC (fig. 2, A and B, green). Conformational changes due to desensitization may alter the TMD intrasubunit pocket and introduce motional restriction on residues lining the pocket, including residues 265 and 308.

We further investigated whether and how propofol binding affected this TMD pocket. In the absence of agonist, propofol binding induced changes in both the ^{19}F NMR linewidth (approximately 50-Hz increase) and the chemical shift (fig. 2, C and D, red), reflecting an alteration in the binding environment and motion of pocket residues. In contrast, adding propofol to the desensitized ELIC produced no change in chemical shift and peak linewidths (fig. 2, E and F, orange). The ^{19}F NMR results are consistent with the finding from the photolabeling experiments that propofol binds to the TMD site in the resting state but not in a desensitized condition (fig. 1).

Temperature coefficients, derived from chemical shifts collected at various temperatures (fig. 2G), also reflect changes in solvent exposure and ligand binding. Residue 265 is closer to the ECD–TMD interface than residue 308 and has a higher probability to be exposed to solvent. Thus, it has a greater temperature coefficient than residue 308 (fig. 2H, solid). We found that temperature coefficients for both residues 265 and 308 decreased in the presence of propofol (fig. 2H, dash), suggesting a plausible solvent-shielding effect on propofol binding. A greater decrease in temperature coefficient on propofol binding in residue 265 than residue 308 is notable, consistent with different solvent accessibilities and shielding effects of these two residues.

Taken together, the ^{19}F NMR results provide supportive evidence for propofol binding to the TMD intrasubunit pocket lined by residues 265 and 308 in the resting state of ELIC.

Functional Relevance of the TMD Pocket to Propofol Inhibition of ELIC

We investigated the functional relevance of propofol binding to the TMD intrasubunit pocket through three sets of experiments. First, compared with propofol inhibition of ELIC (IC_{50} = 30.2 ± 1.1 μM), we found that the M265C and F308C mutants had notable right shifts of their propofol inhibition curves and their IC_{50} values increased to 50.5 ± 1.1 μM and 102.4 ± 1.2 μM, respectively (fig. 3A). Clearly, altering this TMD intrasubunit pocket reduced inhibitory effects of propofol at a given concentration. Second, we noticed that preincubating oocytes with propofol or AziP*m* increased the inhibitory effect on ELIC (fig. 3B). The preincubation data alone cannot differentiate whether propofol binding to the TMD or the ECD predominates the ELIC inhibition but indicates that propofol binds ELIC in the resting state and stabilizes the closed-channel conformation, thereby preventing the channels from opening. Although the preincubation data echo the results that AziP*m* and propofol bind to the TMD intrasubunit pocket favorably in the resting state (figs. 1 and 2), the propofol labeling of Y102 in the ECD (fig. 1D) complicates the source of additional inhibition through preincubation. Thus, we used the ELIC-GABA$_A$R chimera to determine the role of the TMD in propofol inhibition of ELIC. ELIC-GABA$_A$R has the ECD of ELIC and the TMD of the human α1β3GABA$_A$R. As expected, the agonist propylamine of ELIC activates ELIC-GABA$_A$R (fig. S5C, Supplemental Digital Content 1, http://links.lww.com/ALN/B239). The ELIC-GABA$_A$R chimera also shows inhibition by picrotoxin and zinc (fig. S5D, Supplemental Digital Content 1, http://links.lww.com/ALN/B239), which has been observed on both GABA$_A$Rs and ELIC.[39–43] An intriguing difference between ELIC-GABA$_A$R and ELIC, however, lies in their functional responses to propofol. At the same effective agonist concentrations, propofol

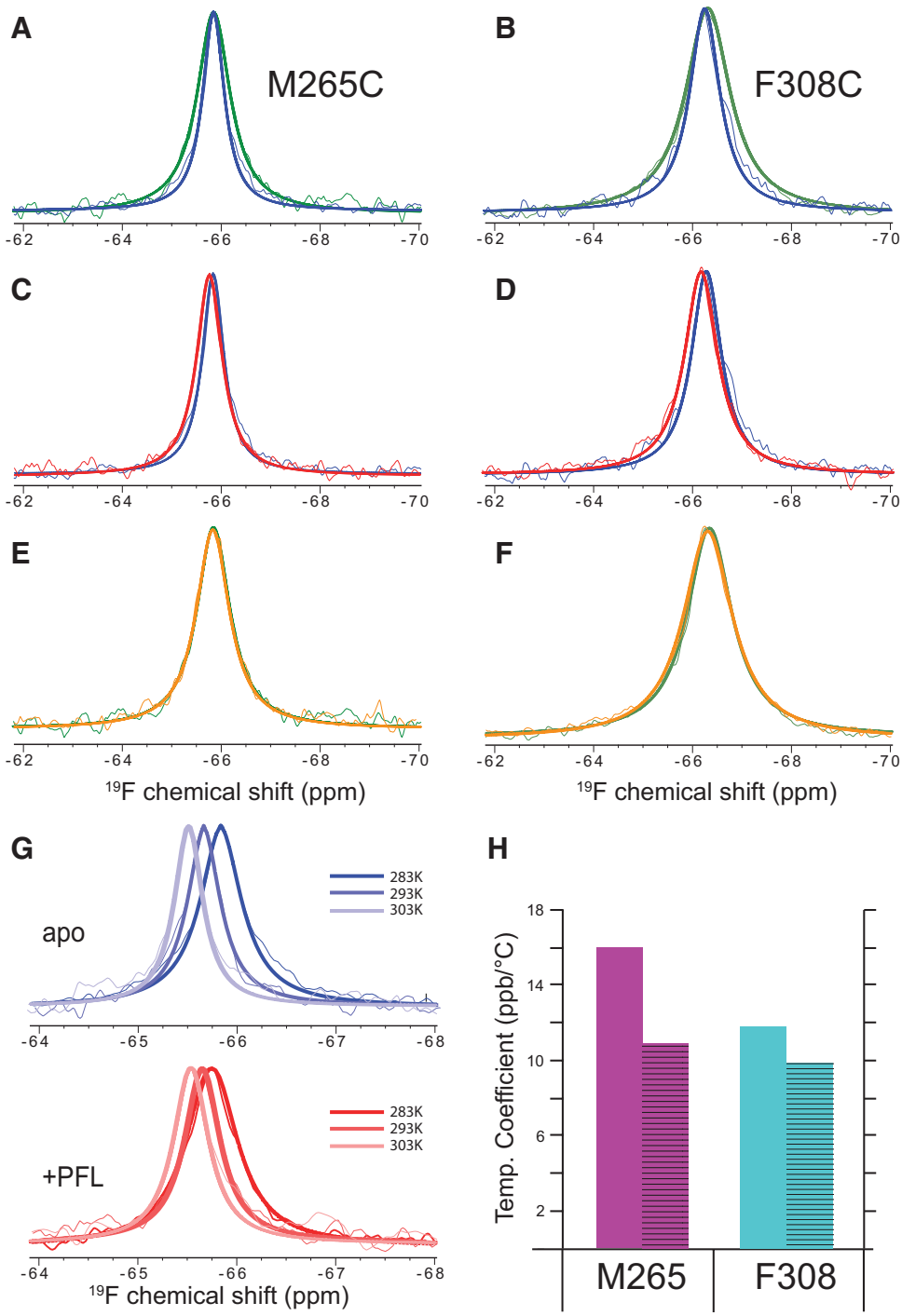

Fig. 2. ^{19}F NMR showed propofol binding to the transmembrane domain intrasubunit pocket of pentameric ligand-gated ion channel from *Erwinia chrysanthemi* (ELIC) only in the resting state. (*A* and *B*) The agonist propylamine (18 mM) binding (green) broadened the ^{19}F NMR linewidths of sites 265 and 308 compared with the linewidths in the absence of agonist (*blue*). (*C* and *D*) The addition of propofol (120 μM) caused downfield shift and approximately 50-Hz increase in the linewidth of the ^{19}F NMR peaks (*red*) compared with that in the apo ELIC (*blue*). (*E* and *F*) Under desensitized conditions (*green*), no change was observed in the ^{19}F NMR spectra upon the addition of propofol (*orange*). (*G*) Temperature dependence of the ^{19}F chemical shift for site 265 in the absence (*blue*) and presence (*red*) of propofol. (*H*) Temperature coefficients calculated based on the experiments as shown in (*G*) for sites 265 (*magenta*) and 308 (*cyan*) in the absence (*solid*) and presence (*hash*) of propofol. PFL = propofol.

inhibits the currents of ELIC but potentiates the currents of ELIC-GABA$_A$R (fig. 3C). ELIC-GABA$_A$R clearly resembles GABA$_A$Rs in response to propofol modulation,[44] even though propofol likely binds to the ECD of ELIC-GABA$_A$R as it does to ELIC. The transformation from propofol inhibition to potentiation by replacing the TMD suggests that

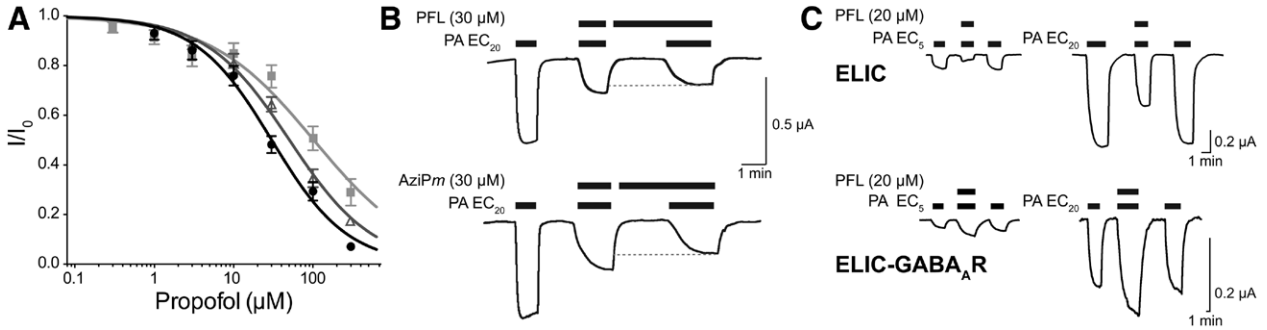

Fig. 3. Functional relevance of the transmembrane domain (TMD) intrasubunit propofol-binding pocket. (*A*) Mutations to the TMD intrasubunit pocket decreased propofol sensitivity. Propofol inhibition curves were collected at the EC_{20} concentration of propylamine (PA), and data were fit to the Hill equation. IC_{50} values are 50.5 ± 1.3 μM for M265C (*open triangles*), 102.4 ± 1.2 μM for F308C (*squares*), and 30.2 ± 1.1 μM for pentameric ligand-gated ion channel from *Erwinia chrysanthemi* (ELIC) (*circles*). Data are for n ≥ 5 oocytes and error bars represent SEM. (*B*) Representative traces showing that preincubation of oocytes with propofol (*top*) or a light-activated derivative of propofol (AziP*m*) (*bottom*) increased the maximum inhibition of ELIC. (*C*) Representative traces comparing propofol inhibition of ELIC and potentiation of the ELIC-$GABA_AR$ chimera at EC_5 and EC_{20} of the agonist PA. Replacing the ELIC-TMD with that of α1β3$GABA_AR$ drastically changed the channels' functional response to propofol. The result highlights the functional relevance of the TMD-binding site. More functional data are provided in figure S5 (Supplemental Digital Content 1, http://links.lww.com/ALN/B239). GAB_AR = γ-aminobutyric acid receptor; PA = propylamine; PFL = propofol.

propofol binding to the TMD dominates the functional consequences. Such a determinant role of the TMD was also observed in our previous study with the ELIC-α7nAChR chimera, which shows the same functional response to propofol as the native α7nAChR but is markedly different from ELIC.[29]

We also notice that the different response to propofol between ELIC-$GABA_AR$ and ELIC remains even at a high effective agonist concentration (greater than or equal to EC_{50}), where ELIC-$GABA_AR$ shows diminishing potentiation by propofol (fig. S5C, Supplemental Digital Content 1, http://links.lww.com/ALN/B239) but ELIC is still inhibited substantially by propofol.[13]

Molecular Details of Propofol Binding Revealed by MD Simulations

We performed MD simulations of ELIC (PDB code: 3RQU)[28] in the absence and presence of propofol bound to the TMD site suggested by photolabeling and ^{19}F NMR. Most propofol molecules docked into the TMD pockets remained stable over the course of two parallel MD simulations (fig. S6A and S6B, Supplemental Digital Content 1, http://links.lww.com/ALN/B239). Residues within 3 Å of propofol are both hydrophobic and hydrophilic, forming an amphipathic-binding pocket (fig. 4A). In the absence of propofol, water molecules occupied the pocket in the simulations (fig. 4B). Propofol was also docked to the photolabeling-predicted ECD sites involving residues Y102, G98, and F95 (fig. S6C, S6D, and S6E, Supplemental Digital Content 1, http://links.lww.com/ALN/B239). Most propofol molecules in the ECD were stable in their docked sites over the course of the MD simulations, but propofol near residue G98 showed unstable binding in one of the MD simulations (fig. S6D, Supplemental Digital Content 1, http://links.lww.com/ALN/B239).

We compared root mean square fluctuations of ELIC in the three simulation systems and noticed several results (fig. 4, C and D). Propofol binding to the TMD intrasubunit pocket reduced motional flexibility of the upper half of the TM2 and TM3 helices (fig. 4C and fig. S7A and S7B, gray box, Supplemental Digital Content 1, http://links.lww.com/ALN/B239). The reduced flexibility in this region may affect the pore conformational transitions from the resting to other functional states. For the same TM2 and TM3 regions, independent simulations with propofol bound only to the ECD (fig. 4D and fig. S7C and S7D, gray box, Supplemental Digital Content 1, http://links.lww.com/ALN/B239) displayed nearly the same root mean square fluctuations as observed in the simulations of APO ELIC. It is also worth mentioning that TM4 showed a much higher flexibility than the other TM helices (fig. 4C-D and fig. S7, Supplemental Digital Content 1, http://links.lww.com/ALN/B239). A structural comparison shows that the TM4 helix tilts outward by approximately 7° upon propofol binding (fig. S8, Supplemental Digital Content 1, http://links.lww.com/ALN/B239). This inherent flexibility of TM4 may contribute to the conformational plasticity of the intrasubunit pocket, thereby allowing this pocket to be amenable to drug-binding events.

Discussion

We have taken multiple approaches and determined a functionally relevant propofol-binding site in the TMD of ELIC. Interestingly, this newly identified TMD intrasubunit propofol-binding pocket in ELIC overlaps with the sites reported for binding propofol and other anesthetics in GLIC[10,14] and nAChRs.[5,7,11,24–26] The repeat occurrence of this location for binding anesthetics in different cation-conducting pLGICs suggests that this is a common pocket

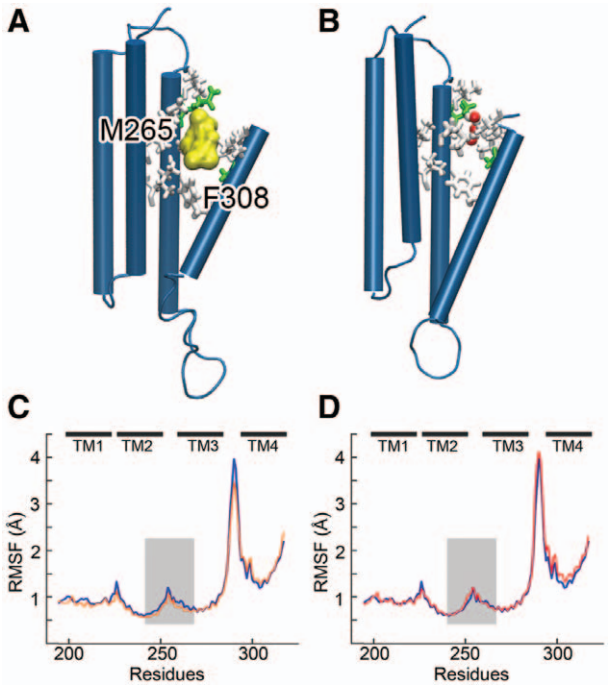

Fig. 4. Propofol binding visualized by molecular dynamic (MD) simulations. (*A*) The transmembrane domain (TMD) intrasubunit binding pocket contains both hydrophobic (*white*) and hydrophilic (*green*) residues. The docked propofol is shown in *yellow* surface. (*B*) Water molecules (*red*) occupied the TMD intrasubunit pocket in the absence of propofol in MD simulations. (*C*) Comparisons of root mean square fluctuations (RMSFs) calculated from MD simulations for APO pentameric ligand-gated ion channel from *Erwinia chrysanthemi* (ELIC) (*blue*) *versus* ELIC bound with propofol in the TMD intrasubunit pocket (*orange*) or (*D*) *versus* ELIC bound with propofol in the extracellular domain (*red*). The *gray box* in (*C*) highlights reduction of motional flexibility in the TM2 and TM3 helices in the presence of propofol. The same region in (*D*) shows little change. More details are provided in figures S6 and S7 (Supplemental Digital Content 1, http://links.lww.com/ALN/B239).

for mediating inhibitory effects. Note that such an anesthetic inhibitory site in the TMD has been reported only for the cation-conducting pLGICs.[5,7,10,11,14,24–26] Several features of this intrasubunit pocket may contribute to the functional relevance of anesthetic binding to the pocket. This pocket is bordered by the ECD and TMD interface that is known to play an important role in allosteric modulation of channel functions.[29] This pocket is also behind the pore-lining TM2 helix. Anesthetic binding could reduce TM2 flexibility, as shown in figure 4C, and thereby potentially add resistance to conformational transitions between functional states. In addition, the amphipathic nature of the TMD intrasubunit pocket (fig. 4A) is favored by general anesthetics.[45,46] Furthermore, the highly flexible TM4 helix (fig. 4C and fig. S7, Supplemental Digital Content 1, http://links.lww.com/ALN/B239) provides plasticity to the pocket and allows it to accommodate anesthetics of varied molecular sizes. Altogether, this pocket is both functionally relevant for anesthetic inhibition and structurally feasible for hosting a variety of anesthetic molecules.

Our study has demonstrated that propofol binding to the TMD intrasubunit pocket depends on the functional states of ELIC. Specifically, propofol binds to the TMD pocket in the resting state of ELIC but not in a desensitized state. The difference in binding between the two states implies a considerable change in the pocket conformation from one state to another. Our recent ^{19}F NMR and ESR studies[31] found widening of the extracellular pore entrance underlying ELIC desensitization that was associated with the outward tilting of the upper region of the TM2 helix. Such tilting could be one of the changes induced by desensitization that alters the TMD intrasubunit drug-binding pocket and disrupts propofol binding. The preferential binding of propofol to a functional state varies among pLGICs. In the case of GLIC, propofol binding to the TMD intrasubunit pocket was observed at a low pH,[10,14] a condition that renders GLIC either open or desensitized. For a muscle-type nAChR, propofol bounds to the TMD intrasubunit pocket of the δ subunit only under desensitization conditions.[11] It is axiomatic that the preference of a functional state for propofol binding is determined by the pocket conformation in that given state. The discovery that propofol binds to the TMD intrasubunit site in the resting state of ELIC suggests an inhibitory mechanism, in which anesthetic binding to a pLGIC in the resting state stabilizes a closed-channel conformation and thereby adds resistance to channel activation.

The consensus that multiple anesthetic-binding sites exist in a given pLGIC has emerged in recent years.[5,12,16] Among multiple anesthetic-binding sites found in a protein, it is necessary to determine which site is relevant to the functional modulation by anesthetics, either inhibition or potentiation. In the current study with ELIC, we have demonstrated an effective approach of using an engineered chimera to differentiate a functionally relevant propofol-binding site in the TMD from other binding sites in the ECD. The observed propofol potentiation of ELIC-GABA$_A$R *versus* the propofol inhibition of ELIC highlights a critical role of the TMD in channel functional modulation by propofol. We previously also made an ELIC-α7nAChR chimera, which has the ECD of ELIC and the TMD of α7nAChR.[29] We found that ELIC-α7nAChR was as insensitive to propofol as α7nAChR.[29] Because ELIC, ELIC-α7nAChR, and ELIC-GABA$_A$R have the same ECD, their drastically different functional responses to propofol binding must predominantly result from the differences in the TMD, even though we do not rule out the possibility that the propofol molecules bound to the ECD also participate in functional modulation with a much smaller impact. Separate studies are required to find out where propofol binds to the TMD of ELIC-α1β3GABA$_A$R and ELIC-α7nAChR, as well as how propofol generates functional effects on these chimeras different from the effect on ELIC, although propofol has been reported to bind to the TMD intersubunit pockets of α1β3GABA$_A$R.[12] Within the scope of the current study, these

chimeras have served the purpose of assisting in determining which site is more functionally relevant. The chimera results also added compelling evidence to support the hypothesis that most functionally relevant sites for anesthetic binding are located in the TMD, even though exceptions exist.[15] Based on the findings from the current and previously published studies,[5,7,10,11,14] we anticipate the emergence of additional evidence to support the existence of a common anesthetic inhibitory site in cation-conducting pLGICs.

Acknowledgments

The authors thank Tommy S. Tillman, Ph.D., Department of Anesthesiology, University of Pittsburgh School of Medicine, Pittsburgh, Pennsylvania, for his help in functional measurements; and Marta Wells, B.S., Departments of Anesthesiology and Computational and Systems Biology, University of Pittsburgh School of Medicine, for her help in the initial docking studies.

M.N.K. was supported by the National Institutes of Health (NIH, Bethesda, Maryland) Ruth L. Kirschstein National Service Award (T32GM075770 to Y.X.). The MD simulations were supported, in part, by the National Science Foundation (Arlington, Virginia) through TeraGrid resources (TG-MCB050030N). The research was supported by funding from the NIH (R01GM056257, R01GM066358, and P01GM055876).

Competing Interests

The authors declare no competing interests.

Correspondence

Address correspondence to Dr. Tang: Department of Anesthesiology, 2049 BST3, 3501 Fifth Avenue, Pittsburgh, Pennsylvania 15260. ptang@pitt.edu.

References

1. Franks NP, Lieb WR: Molecular and cellular mechanisms of general anaesthesia. Nature 1994; 367:607–14
2. Forman SA, Miller KW: Anesthetic sites and allosteric mechanisms of action on Cys-loop ligand-gated ion channels. Can J Anaesth 2011; 58:191–205
3. Eckenhoff RG, Johansson JS, Wei H, Carnini A, Kang B, Wei W, Pidikiti R, Keller JM, Eckenhoff MF: Inhaled anesthetic enhancement of amyloid-beta oligomerization and cytotoxicity. Anesthesiology 2004; 101:703–9
4. Jevtovic-Todorovic V, Hartman RE, Izumi Y, Benshoff ND, Dikranian K, Zorumski CF, Olney JW, Wozniak DF: Early exposure to common anesthetic agents causes widespread neurodegeneration in the developing rat brain and persistent learning deficits. J Neurosci 2003; 23:876–82
5. Bondarenko V, Mowrey D, Liu LT, Xu Y, Tang P: NMR resolved multiple anesthetic binding sites in the TM domains of the α4β2 nAChR. Biochim Biophys Acta 2013; 1828:398–404
6. Bondarenko V, Mowrey DD, Tillman TS, Seyoum E, Xu Y, Tang P: NMR structures of the human α7 nAChR transmembrane domain and associated anesthetic binding sites. Biochim Biophys Acta 2014; 1838:1389–95
7. Mowrey DD, Liu Q, Bondarenko V, Chen Q, Seyoum E, Xu Y, Wu J, Tang P: Insights into distinct modulation of α7 and α7β2 nicotinic acetylcholine receptors by the volatile anesthetic isoflurane. J Biol Chem 2013; 288:35793–800
8. Tillman T, Cheng MH, Chen Q, Tang P, Xu Y: Reversal of ion-charge selectivity renders the pentameric ligand-gated ion channel GLIC insensitive to anaesthetics. Biochem J 2013; 449:61–8
9. Chen Q, Cheng MH, Xu Y, Tang P: Anesthetic binding in a pentameric ligand-gated ion channel: GLIC. Biophys J 2010; 99:1801–9
10. Chiara DC, Gill JF, Chen Q, Tillman T, Dailey WP, Eckenhoff RG, Xu Y, Tang P, Cohen JB: Photoaffinity labeling the propofol binding site in GLIC. Biochemistry 2014; 53:135–42
11. Jayakar SS, Dailey WP, Eckenhoff RG, Cohen JB: Identification of propofol binding sites in a nicotinic acetylcholine receptor with a photoreactive propofol analog. J Biol Chem 2013; 288:6178–89
12. Jayakar SS, Zhou X, Chiara DC, Dostalova Z, Savechenkov PY, Bruzik KS, Dailey WP, Miller KW, Eckenhoff RG, Cohen JB: Multiple propofol-binding sites in a γ-aminobutyric acid type A receptor (GABAAR) identified using a photoreactive propofol analog. J Biol Chem 2014; 289:27456–68
13. Chen Q, Kinde MN, Arjunan P, Wells MM, Cohen AE, Xu Y, Tang P: Direct pore binding as a mechanism for isoflurane inhibition of the pentameric ligand-gated ion channel ELIC. Sci Rep 2015; 5:13833
14. Nury H, Van Renterghem C, Weng Y, Tran A, Baaden M, Dufresne V, Changeux JP, Sonner JM, Delarue M, Corringer PJ: X-ray structures of general anaesthetics bound to a pentameric ligand-gated ion channel. Nature 2011; 469:428–31
15. Pan J, Chen Q, Willenbring D, Mowrey D, Kong XP, Cohen A, Divito CB, Xu Y, Tang P: Structure of the pentameric ligand-gated ion channel GLIC bound with anesthetic ketamine. Structure 2012; 20:1463–9
16. Spurny R, Billen B, Howard RJ, Brams M, Debaveye S, Price KL, Weston DA, Strelkov SV, Tytgat J, Bertrand S, Bertrand D, Lummis SC, Ulens C: Multisite binding of a general anesthetic to the prokaryotic pentameric *Erwinia chrysanthemi* ligand-gated ion channel (ELIC). J Biol Chem 2013; 288:8355–64
17. Mowrey D, Cheng MH, Liu LT, Willenbring D, Lu X, Wymore T, Xu Y, Tang P: Asymmetric ligand binding facilitates conformational transitions in pentameric ligand-gated ion channels. J Am Chem Soc 2013; 135:2172–80
18. Willenbring D, Liu LT, Mowrey D, Xu Y, Tang P: Isoflurane alters the structure and dynamics of GLIC. Biophys J 2011; 101:1905–12
19. Brannigan G, LeBard DN, Hénin J, Eckenhoff RG, Klein ML: Multiple binding sites for the general anesthetic isoflurane identified in the nicotinic acetylcholine receptor transmembrane domain. Proc Natl Acad Sci U S A 2010; 107:14122–7
20. Forman SA, Miller KW, Yellen G: A discrete site for general anesthetics on a postsynaptic receptor. Mol Pharmacol 1995; 48:574–81
21. Dilger JP, Brett RS, Lesko LA: Effects of isoflurane on acetylcholine receptor channels. 1. Single-channel currents. Mol Pharmacol 1992; 41:127–33
22. Zhou QL, Zhou Q, Forman SA: The n-alcohol site in the nicotinic receptor pore is a hydrophobic patch. Biochemistry 2000; 39:14920–6
23. Nirthanan S, Garcia G III, Chiara DC, Husain SS, Cohen JB: Identification of binding sites in the nicotinic acetylcholine receptor for TDBzl-etomidate, a photoreactive positive allosteric effector. J Biol Chem 2008; 283:22051–62
24. Chiara DC, Hong FH, Arevalo E, Husain SS, Miller KW, Forman SA, Cohen JB: Time-resolved photolabeling of the nicotinic acetylcholine receptor by [3H]azietomidate, an open-state inhibitor. Mol Pharmacol 2009; 75:1084–95
25. HamoudaAK,StewartDS,HusainSS,CohenJB:Multipletransmembrane binding sites for p-trifluoromethyldiazirinyl-etomidate, a

photoreactive Torpedo nicotinic acetylcholine receptor allosteric inhibitor. J Biol Chem 2011; 286:20466–77

26. Chiara DC, Dangott LJ, Eckenhoff RG, Cohen JB: Identification of nicotinic acetylcholine receptor amino acids photolabeled by the volatile anesthetic halothane. Biochemistry 2003; 42:13457–67
27. Hilf RJ, Dutzler R: X-ray structure of a prokaryotic pentameric ligand-gated ion channel. Nature 2008; 452:375–9
28. Pan J, Chen Q, Willenbring D, Yoshida K, Tillman T, Kashlan OB, Cohen A, Kong XP, Xu Y, Tang P: Structure of the pentameric ligand-gated ion channel ELIC cocrystallized with its competitive antagonist acetylcholine. Nat Commun 2012; 3:714
29. Tillman TS, Seyoum E, Mowrey DD, Xu Y, Tang P: ELIC-α7 Nicotinic acetylcholine receptor (α7nAChR) chimeras reveal a prominent role of the extracellular-transmembrane domain interface in allosteric modulation. J Biol Chem 2014; 289:13851–7
30. Hall MA, Xi J, Lor C, Dai S, Pearce R, Dailey WP, Eckenhoff RG: m-Azipropofol (AziPm) a photoactive analogue of the intravenous general anesthetic propofol. J Med Chem 2010; 53:5667–75
31. Kinde MN, Chen Q, Lawless MJ, Mowrey DD, Xu J, Saxena S, Xu Y, Tang P: Conformational changes underlying desensitization of the pentameric ligand-gated ion channel ELIC. Structure 2015; 23:995–1004
32. Liu JJ, Horst R, Katritch V, Stevens RC, Wüthrich K: Biased signaling pathways in β2-adrenergic receptor characterized by 19F-NMR. Science 2012; 335:1106–10
33. Mehta VD, Kulkarni PV, Mason RP, Constantinescu A, Antich PP: Fluorinated proteins as potential 19F magnetic resonance imaging and spectroscopy agents. Bioconjug Chem 1994; 5:257–61
34. Morris GM, Huey R, Lindstrom W, Sanner MF, Belew RK, Goodsell DS, Olson AJ: AutoDock4 and AutoDockTools4: Automated docking with selective receptor flexibility. J Comput Chem 2009; 30:2785–91
35. Phillips JC, Braun R, Wang W, Gumbart J, Tajkhorshid E, Villa E, Chipot C, Skeel RD, Kalé L, Schulten K: Scalable molecular dynamics with NAMD. J Comput Chem 2005; 26:1781–802
36. Best RB, Zhu X, Shim J, Lopes PE, Mittal J, Feig M, Mackerell AD Jr: Optimization of the additive CHARMM all-atom protein force field targeting improved sampling of the backbone φ, ψ and side-chain χ(1) and χ(2) dihedral angles. J Chem Theory Comput 2012; 8:3257–73
37. Darden T, York D, Pedersen L: Particle mesh Ewald—An N.Log(N) method for Ewald sums in large systems. J Chem Phys 1993;98:10089–92
38. Kitevski-LeBlanc JL, Prosser RS: Current applications of 19F NMR to studies of protein structure and dynamics. Prog Nucl Magn Reson Spectrosc 2012; 62:1–33
39. Krishek BJ, Moss SJ, Smart TG: A functional comparison of the antagonists bicuculline and picrotoxin at recombinant GABAA receptors. Neuropharmacology 1996; 35:1289–98
40. Thompson AJ, Alqazzaz M, Price KL, Weston DA, Lummis SC: Phenylalanine in the pore of the Erwinia ligand-gated ion channel modulates picrotoxinin potency but not receptor function. Biochemistry 2014; 53:6183–8
41. Marabelli A, Lape R, Sivilotti L: Mechanism of activation of the prokaryotic channel ELIC by propylamine: A single-channel study. J Gen Physiol 2015; 145:23–45
42. Zimmermann I, Marabelli A, Bertozzi C, Sivilotti LG, Dutzler R: Inhibition of the prokaryotic pentameric ligand-gated ion channel ELIC by divalent cations. PLoS Biol 2012; 10:e1001429
43. Smart TG, Moss SJ, Xie X, Huganir RL: GABAA receptors are differentially sensitive to zinc: Dependence on subunit composition. Br J Pharmacol 1991; 103:1837–9
44. Hales TG, Lambert JJ: The actions of propofol on inhibitory amino acid receptors of bovine adrenomedullary chromaffin cells and rodent central neurones. Br J Pharmacol 1991; 104:619–28
45. Xu Y, Tang P: Amphiphilic sites for general anesthetic action? Evidence from 129Xe-[1H] intermolecular nuclear Overhauser effects. Biochim Biophys Acta 1997; 1323:154–62
46. Tang P, Yan B, Xu Y: Different distribution of fluorinated anesthetics and nonanesthetics in model membrane: A 19F NMR study. Biophys J 1997; 72:1676–82